

On the use of diagnostic forces applied on rotating machines for crack detection

Nicolò Bachschmid², Aldemir Ap Cavalini Jr¹, Tobias Souza Morais¹, Valder Steffen Jr¹

¹LMEst - Laboratory of Mechanics and Structures, Federal University of Uberlândia, School of Mechanical Engineering, Av. João Naves de Ávila, 2121, Uberlândia, MG, 38408-196, Brazil.

²Department of Mechanical Engineering, Politecnico di Milano, Via La Masa 1, Milano, 20156, Italy.

nicolo.bachschmid@polimi.it, aacjunior@ufu.br, tobias@ufu.br, vsteffen@ufu.br

Abstract

The authors have analysed in a previous paper the use of the combinational resonance vibrations, excited by diagnostic forces at suitable frequencies, for detecting the crack signature. The conditions where this technique can be applied successfully are analysed in this paper. Applying diagnostic forces to real industrial machinery is feasible only if the machine is equipped with an electromagnetic exciter for vibration control or with magnetic bearing. In this case, considering an industrial machine, generally equipped with oil film bearings, with well damped critical speeds, it is necessary to know which force and which frequency is required for generating a measurable peak as combination resonance. In this paper, a quasi linear approach based on the harmonic balance in the frequency domain is presented that allows to derive simple expressions of the equivalent forces which generate combination frequency vibrations, as well as their resulting amplitudes. It will be shown that these forces are proportional to the crack induced stiffness variation and to the vibration amplitudes generated by the diagnostic force in correspondence of the crack. These simple expressions allow to evaluate the possibility and effectiveness of this crack identification methodology based on diagnostic force application. In the inverse problem, these expressions could be further used in a model based approach for identifying cracks from measured combination frequency vibrations.

1 Introduction

Shaft crack detection is an important issue in rotor dynamics. Early recognition of cracks in rotating shafts can prevent catastrophic failures. Thus, accurate monitoring is required for industrial rotating machinery such as turbines, compressors, pumps, and generators. There are several SHM techniques proposed in the literature for crack detection in rotating machines mainly based on vibration measurements. Although widely used in industry, when applied under non-ideal conditions such techniques can only detect cracks that eventually have already spread significantly along the cross section of the shaft (usually above 40% of its diameter). Therefore, currently, the researchers' attention is turning to more sophisticated methods capable of identifying incipient cracks (cracks that spread up to 25% of shaft diameter), that are hardly observable in classical vibration analysis during normal operating conditions.

Various structural health monitoring (SHM) techniques devoted to crack detection in rotating machines have been proposed in the last decade. Changes in 1X and 2X vibration amplitudes and phases are considered the primary indicators of crack presence (see e.g. [1], [2]). Among several different approaches described in a rich literature for crack detection in rotating shafts, the SHM methodologies that use harmonic excitations as diagnostic forces has attracted the attention of several researchers and two interesting results are here recalled. The purpose of applying the diagnostic forces in a cracked shaft at different frequencies from the rotation speed is to excite combination frequency vibrations that are measurable when the

combination frequency equals one of the natural frequencies of the system. These conditions are then called combination resonances.

A theoretical analysis considering a simple rotor model with 2 degrees of freedom containing a breathing crack is presented in [3]. The method of multiple scales was used to solve the equations of motion of the system, in which the stiffness of the shaft was affected by the nonlinearity (i.e., the breathing crack). The so-called combination resonances were defined in the context of rotating cracked shafts. It was shown that the vibration amplitudes associated with the combination resonances are directly proportional to the time dependent stiffness, i.e., to the crack depth. An accurate numerical and analytical analyses on a cracked Jeffcott rotor is presented further in [4]. The stiffness of the cracked shaft has been modelled by using two different approaches, namely: i) a piecewise linear stiffness and ii) by using power series. The effects of the excitation intensity (diagnostic forces) on the forward and backward whirl vibration responses of the rotor system at the combination resonances were evaluated according to the crack severity. An experimental validation of the proposed method was also presented, in which the combination resonances were demonstrated on the vibration responses of the considered rotating machine. More recently the possibility of identifying the severity of transverse cracks (i.e., position and depth) in rotating shafts by using the so-called diagnostic forces and combination resonances has been analysed in [5]. The frequencies of the diagnostic forces were determined by using the method of multiple scales. This approach was applied to a rotor test rig model composed by a horizontal shaft, two rigid discs, two self-alignment ball bearings, and an electromagnetic actuator used to introduce the harmonic excitations. The horizontal vibration responses of the rotating machine were measured by using displacement sensors located close to the discs. The dynamic behaviour of the system was investigated considering both the breathing and open crack models. The crack models were formulated from the Mayes model (breathing crack described in [6]) combined with the linear fracture mechanics approach (breathing and open cracks). Vibration responses in the time domain have been determined for different crack positions and depths. In a given test case, the proposed methodology was able to identify, with good accuracy, the severity of the crack by using the Differential Evolution optimization method (described in [7]). In that contribution, constant rotation speed and various diagnostic excitations at frequencies suitable for exciting two combination resonances were considered.

However, the problem consists in determining the amplitude and frequency of the diagnostic forces to generate measurable peaks on the vibration spectrum at the combination resonances. This is an important issue, mainly when the proposed technique is applied to industrial machinery, due to the limitations regarding the applicable force amplitude and position.

Therefore, the vibration response of the system at the combination resonances depends on the damping, the location of the crack along the shaft, the locations where the diagnostic forces are applied, and the amplitude of the diagnostic forces. In this paper, the dynamic behaviour of a cracked rotating shaft is analysed to determine the most favourable conditions to apply the mentioned SHM technique by using the harmonic balance approach. This quasi-linear methodology is able to determine the vibration amplitudes and phase angles at the combination resonances generated by the presence of the crack when external diagnostic forces are applied to the rotor system. Additionally, the obtained results are compared with the ones determined from the trapezoidal rule integration scheme, which was coupled with the Newton-Raphson iterative method for nonlinear analysis, used also in [5].

2 Combination frequency vibrations

The purpose of applying to a cracked rotating shaft diagnostic forces at frequencies Ω_d different from rotational speed frequency Ω , consists in exciting “combination frequency vibrations” at frequencies which are combinations of the two frequencies, that appear only in the presence of a transverse crack. In order to emphasize the occurrence of the combination frequency vibrations, it is useful to exploit the possibility of resonant conditions when one of the combination frequencies equals one of the natural frequencies of the shaft. This condition is then called combinational resonance. The high magnification factor in resonance allows then to distinguish the resonance peak from other vibration components and from noise. The natural frequencies of the shaft must be known so that the diagnostic force frequency can be selected in advance. But, which should be the diagnostic force amplitude in order to generate in the measuring points a

measurable peak in the vibration spectrum? This is an important issue when this technique should be applied to industrial machinery where limitations in applicable force amplitude may exist. The response of the system depends on the damping, on the location of the crack in the shaft and on the location where the diagnostic force is applied.

Applying diagnostic forces to real industrial machinery is feasible only if the machine is equipped with an electromagnetic exciter for vibration control or with magnetic bearing, or if at the design stage of the machine the possibility of applying electromagnetic forces in at least one location of the shaft-line has been foreseen.

In this case, considering an industrial machine, generally equipped with oil film bearings, operating at rated speed, with well damped critical speeds, it would be interesting to know in advance which force is required for generating a measurable peak as combination resonance, in the proximity probes that are installed generally in correspondence of the bearings.

It will be shown that combination frequency vibrations can be calculated quite easily assuming linearity of the system and applying the harmonic balance approach in the frequency domain.

Combination frequency vibrations are generated already by the rotating unbalance, combined to the rotating crack, but combination resonance conditions can hardly be attained since rotational speed cannot be changed ad libitum. The frequency of the external diagnostic force can instead be changed generally in a wide range according to the specification of the actuator, so that resonant conditions can be attained. The combination frequency vibration amplitudes depend on the crack induced stiffness variation and on the vibration amplitudes generated by the diagnostic force in correspondence of the crack. In a first step the vibrations generated by the diagnostic force in correspondence of the crack are calculated assuming the shaft in its original condition without crack. Or more accurately introducing in the stiffness matrix of the shaft the mean stiffness of the cracked beam element, instead of the full stiffness of the un-cracked beam element. Then the equivalent forces can be evaluated and applied to the finite element model (FE model) of the shaft, and the combination frequency vibrations are calculated.

The vibration amplitudes will then be compared to the vibrations of the cracked rotor computed with the nonlinear approach in the time domain. The model used for the comparison is that of [5].

Since in reality the excitation of combination frequency vibrations is a nonlinear effect in a linear system, the proposed approach is a quasi-linear approach that may require some iteration in the evaluation of the vibrations.

Also, the inverse problem of identification of crack depth and position from combination frequency vibrations, and from other crack related symptoms, by use of a well-established model based diagnostic approach in the frequency domain [1], is easily feasible since these vibrations, according to the present approach, are generated by some equivalent external forces that depend of the crack depth and of the diagnostic excitation strength.

Cracks may be always open cracks or breathing cracks. Shafts affected by open cracks behave according linear systems with parametric excitation. Shafts with breathing cracks may also be considered linear systems when breathing is weight dominated, as it occurs in horizontal rotating heavy shafts. When breathing is dominated by vibrations as it may occur in vertical shafts or in horizontal light and weakly damped shafts, then the system becomes really non-linear, as shown in [1].

In this paper, we restrict the analysis to linear systems with parametric excitation. Thus, for modelling the crack the FLEX model proposed in [1] has been used.

2.1 Development of the equation of motion

Let's assume a FE model for the system composed by the shaft, the bearings and the supporting structure, in which the crack is modelled (according to [1]) by a small "equivalent" axially unsymmetrical beam element that generates different stiffness according to the rotating principal axes, as shown in Fig. 1. This axial asymmetry and the length l_c of the equivalent beam are functions of the depth of the crack.

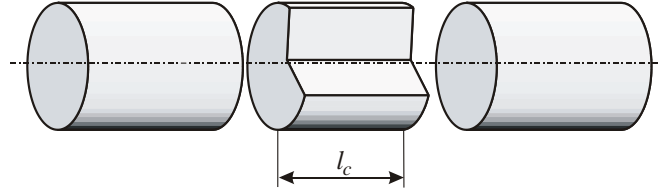


Figure 1: Cracked element configuration (from [1])

With reference to a fixed coordinate system the stiffness of the cracked beam element becomes variable function of the angular position of the shaft. As said before this result is valid for open cracks and for so called weight dominated breathing cracks, in which the opening and closing of the crack during one rotation is forced by the shaft weight. This condition is generally satisfied for horizontal axis industrial machinery or laboratory test rigs. If this is not the case, as in vertical shafts or lightly loaded and poorly damped shafts, as shown in [1], the crack breathing and the corresponding stiffness then depend on the vibration itself so that the behaviour becomes really non-linear.

Assuming weight dominated breathing, the equation of motion of the shaft can be written as follows:

$$\mathbf{M} \mathbf{x}'' + (\mathbf{R} + \mathbf{Gyr}) \mathbf{x}' + \mathbf{K}(\Omega t) \mathbf{x} = \mathbf{Mg} + \mathbf{U}e^{i\Omega t} + \mathbf{F}_d \cos \Omega_d t \quad (1)$$

where \mathbf{x} is the vector of the system node displacements (4 degrees of freedom per node), \mathbf{M} , \mathbf{R} , and \mathbf{Gyr} are respectively the mass, damping, and gyroscopic matrices, respectively, $\mathbf{K}(\Omega t)$ is the stiffness matrix that includes the stiffness of the cracked beam element (which depends on the angular position of the shaft), \mathbf{x} is the vector of displacements of the nodes of the system, \mathbf{Mg} is the vector of weight forces given by the mass matrix multiplied by gravity vector \mathbf{g} , \mathbf{U} is the unbalance (rotating with shaft), \mathbf{F}_d and Ω_d are, respectively, the diagnostic force amplitude and the frequency of the assumed sinusoidal diagnostic force, and Ω is the shaft rotational frequency.

Once the rotation dependent stiffness $\mathbf{K}(\Omega t)$ is defined, eq. (1) can be solved in the time domain for each rotational speed Ω and diagnostic frequency Ω_d , and all vibration components including the combination frequency components can be found in the vibration spectrum. This has been done e.g. in [5].

In this paper an approximated method, based on a harmonic balance approach, is presented that allows to calculate in the frequency domain all the above components. The advantage of the proposed approach is that simple formulas allow to forecast the amplitude of the excited components, as function of the crack depth, of the diagnostic force amplitude and of the dynamic amplification factor at the combination frequency.

In the inverse problem of crack identification from combination frequency components, the same formulas can be used in a model based identification process in the frequency domain based on a rather robust least square approach.

2.2 Harmonic balance approach development

The periodical stiffness $\mathbf{K}(\Omega t)$ that appears in eq. (1) can be developed as Fourier series, as follows. In the case of an always open non-breathing crack, neglecting some smaller component at higher frequency that appear with the Timoshenko beam model (and not with the Bernoulli beam model), the variable stiffness is composed only by a constant term, the mean stiffness \mathbf{K}_m , and by the second harmonic component $\Delta \mathbf{K}_2$:

$$\mathbf{K}(\Omega t) = \mathbf{K}_m + \Delta \mathbf{K}_2 \cos(2\Omega t + \beta) = \mathbf{K}_m + 1/2(\Delta \mathbf{K}_2 e^{i2\Omega t} + \Delta \mathbf{K}_2^* e^{-i2\Omega t}) \quad (2)$$

(letters in bold indicate complex quantities and star * indicates complex conjugate quantity)

In the case of the breathing crack, all different harmonic components will arise, of which only the first three harmonic components $\Delta \mathbf{K}_1$, $\Delta \mathbf{K}_2$, and $\Delta \mathbf{K}_3$ are significant, besides the constant term \mathbf{K}_m :

$$\mathbf{K}(\Omega t) = \mathbf{K}_m + 1/2 (\Delta \mathbf{K}_1 e^{i\Omega t} + \Delta \mathbf{K}_1^* e^{-i\Omega t}) + 1/2 (\Delta \mathbf{K}_2 e^{i2\Omega t} + \Delta \mathbf{K}_2^* e^{-i2\Omega t}) + 1/2 (\Delta \mathbf{K}_3 e^{i3\Omega t} + \Delta \mathbf{K}_3^* e^{-i3\Omega t}) \quad (3)$$

$\Delta\mathbf{K}_1$ is the complex 1xrev shaft stiffness variation, as it results from Fourier analysis, and $\Delta\mathbf{K}_1^*$ is its complex conjugate. Similarly, for the 2xrev and 3xrev complex components of the stiffness variation, that arise from a breathing crack.

Assuming the system linear, the displacement results from superposition of different components:

$$\text{The static component } \mathbf{x}_{st} = \mathbf{K}_m^{-1} \mathbf{Mg} \quad (4.1)$$

$$\text{The 1xrev component } \mathbf{x}(\Omega t) = X_1 \cos(\Omega t + \alpha) = (\mathbf{X}_1 e^{i\Omega t} + \mathbf{X}_1^* e^{-i\Omega t})/2 \quad (4.2)$$

$$\text{The 2xrev component } \mathbf{x}(2\Omega t) = X_2 \cos(2\Omega t + \beta) = (\mathbf{X}_2 e^{i2\Omega t} + \mathbf{X}_2^* e^{-i2\Omega t})/2 \quad (4.3)$$

$$\text{The 3xrev component } \mathbf{x}(3\Omega t) = X_3 \cos(3\Omega t + \delta) = (\mathbf{X}_3 e^{i3\Omega t} + \mathbf{X}_3^* e^{-i3\Omega t})/2 \quad (4.4)$$

$$\text{The diagnostic frequency component } \mathbf{x}(\Omega_d t) = X_d \cos(\Omega_d t + \varphi) = (\mathbf{X}_d e^{i\Omega_d t} + \mathbf{X}_d^* e^{-i\Omega_d t})/2$$

In the first approximation, the displacement is given by $\mathbf{x}_1 = \mathbf{x}_{st} + \mathbf{x}(\Omega t) + \mathbf{x}(2\Omega t) + \mathbf{x}(3\Omega t) + \mathbf{x}(\Omega_d t)$

Let's consider now the simpler case of the non-breathing open crack. Open cracks are easily obtained in laboratory by a small transverse cut machined in the shaft.

Eq. (1) combined with eq. (2) in this case becomes:

$$\mathbf{M} \mathbf{x}_1'' + (\mathbf{R} + \mathbf{Gyr}) \mathbf{x}_1' + \mathbf{K}_m \mathbf{x}_1 = \mathbf{Mg} + \mathbf{U} e^{i\Omega t} + \frac{1}{2} \mathbf{F}_d (e^{i\Omega_d t} + e^{-i\Omega_d t}) - \frac{1}{2} (\Delta\mathbf{K}_2 e^{i2\Omega t} + \Delta\mathbf{K}_2^* e^{-i2\Omega t}) \mathbf{x}_1 \quad (5)$$

By means of the harmonic balance approach we are able to estimate separately in \mathbf{x}_1 the amplitudes of the components at the different frequencies. The stiffness variation $\Delta\mathbf{K}_2$ is very small with respect to the mean stiffness \mathbf{K}_m , at least when the crack depth is small, therefore we assume for *the 1.st iteration* $\Delta\mathbf{K}_2$ negligible with respect to \mathbf{K}_m . Substituting (4), and separating the dynamic components \mathbf{x}_{1d} from static one \mathbf{x}_{st}

$$\mathbf{x}_{1d} = \mathbf{x}_1 - \mathbf{x}_{st} \quad (6)$$

we obtain:

$$\mathbf{M} \mathbf{x}_{1d}'' + (\mathbf{R} + \mathbf{Gyr}) \mathbf{x}_{1d}' + \mathbf{K}_m \mathbf{x}_{1d} = \mathbf{U} e^{i\Omega t} + \frac{1}{2} \mathbf{F}_d (e^{i\Omega_d t} + e^{-i\Omega_d t}) - \frac{1}{2} (\Delta\mathbf{K}_2 e^{i2\Omega t} + \Delta\mathbf{K}_2^* e^{-i2\Omega t}) (\mathbf{x}_{st} + \mathbf{x}_{1d}) \quad (7)$$

\mathbf{x}_{1d} is generally small with respect to \mathbf{x}_{st} , and can be neglected in the last term of eq. (7) in this initial step. Then following vibration components will be obtained:

$$\mathbf{x}_{1d} = \mathbf{x}_{1d}(\Omega) + \mathbf{x}_{1d}(\Omega_d) + \mathbf{x}_{1d}(2\Omega) \quad (8)$$

2.3 Evaluation of the different component amplitudes

Remember that the variation of stiffness due to the crack $\Delta\mathbf{K}_2$ develop in correspondence of the crack position, consequently also \mathbf{x}_{st} and \mathbf{x}_{1d} in eq. (7) must be evaluated in correspondence of the crack position.

As long as the crack is small the shaft stiffness is affected very little by the crack. In shafts affected by a transverse open crack with a depth of 25% of the diameter, the stiffness variation due to the crack is only $\pm 1\%$ of the mean stiffness, as shown in [1]. In the 1.st step the vibration components and their amplitudes, *disregarding all dynamic amplification factors* that are function of the different frequencies, are as follows:

$$\mathbf{x}_{1d}(\Omega) = \mathbf{X}_1 e^{i\Omega t} \text{ due to the unbalance, where } \mathbf{X}_1 = \mathbf{K}_m^{-1} \mathbf{U} \quad (9.1)$$

$$\mathbf{x}_{1d}(2\Omega) = \frac{1}{2} (\mathbf{X}_2 e^{i2\Omega t} + \mathbf{X}_2^* e^{-i2\Omega t}) \text{ due to the } \Delta\mathbf{K}_2 \text{ of the crack, where } \mathbf{X}_2 = \mathbf{K}_m^{-1} \Delta\mathbf{K}_2 \mathbf{K}_m^{-1} \mathbf{Mg} \quad (9.2)$$

$$\mathbf{x}_{1d}(\Omega d) = 1/2 (\mathbf{X}_d e^{i\Omega d t} + \mathbf{X}_d^* e^{-i\Omega d t}) \text{ due to the diagnostic force, where } \mathbf{X}_d = \mathbf{K}_m^{-1} \mathbf{F}_d \quad (9.3)$$

Now we can refine the solution and calculate the last term in eq. (6), which generates, *as 1.st iteration*, following *additional equivalent exciting forces* which will generate additional vibration components:

a) equivalent force components due to unbalance and crack

$$\mathbf{F}(3\Omega) = 1/2 \Delta \mathbf{K}_2 \mathbf{X}_1 e^{i3\Omega t} \quad \text{and} \quad \mathbf{F}(-\Omega) = 1/2 \Delta \mathbf{K}_2^* \mathbf{X}_1 e^{-i\Omega t} \quad (10.1)$$

b) equivalent force components due to crack only

$$\mathbf{F}(4\Omega) = 1/4 \Delta \mathbf{K}_2 \mathbf{X}_2 e^{i4\Omega t} \quad \text{and} \quad \mathbf{F}(-4\Omega) = 1/4 \Delta \mathbf{K}_2^* \mathbf{X}_2^* e^{-i4\Omega t} \quad (10.2)$$

$$\mathbf{F}(0) = 1/4 \Delta \mathbf{K}_2^* \mathbf{X}_2 \quad \text{and} \quad \mathbf{F}(0) = 1/4 \Delta \mathbf{K}_2 \mathbf{X}_2^* \quad (10.3)$$

c) equivalent force components due to diagnostic force and crack

$$\mathbf{F}(\Omega_d + 2\Omega) = 1/4 \Delta \mathbf{K}_2 \mathbf{X}_d e^{i(2\Omega + \Omega_d)t} \quad \text{and} \quad \mathbf{F}(-\Omega_d - 2\Omega) = 1/4 \Delta \mathbf{K}_2^* \mathbf{X}_d^* e^{-i(2\Omega + \Omega_d)t} \quad (10.4)$$

$$\mathbf{F}(\Omega_d - 2\Omega) = 1/4 \Delta \mathbf{K}_2^* \mathbf{X}_d e^{-i(2\Omega - \Omega_d)t} \quad \text{and} \quad \mathbf{F}(-\Omega_d + 2\Omega) = 1/4 \Delta \mathbf{K}_2 \mathbf{X}_d^* e^{i(2\Omega - \Omega_d)t} \quad (10.5)$$

All these force components will generate additional vibration components that have to be added to the components obtained in the first step. $\mathbf{F}(0)$ generates an additional static deflection, the other forces generate components at frequencies $3\Omega, -\Omega, \pm 4\Omega, \pm(\Omega_d + 2\Omega), \pm(\Omega_d - 2\Omega)$.

Disregarding any dynamic amplification factors the amplitudes of these additional vibration components arising in the 1.st iteration will be equal to the inverse of the stiffness matrix \mathbf{K}_m^{-1} multiplied by the above equivalent force amplitudes.

Thus the resulting vibration components will have *much smaller amplitudes* with respect to the 1.st step vibration component amplitudes, given by (9.1), (9.2) and (9.3), unless their frequencies are close to a natural frequency of the system which would generate high dynamic amplification factors.

As an example, the combination vibration component amplitude at frequency $(\Omega_d + 2\Omega)$, disregarding possible dynamic amplification factors, will result

$$\mathbf{X}(\Omega_d + 2\Omega) = 1/2 \mathbf{K}_m^{-1} \Delta \mathbf{K}_2 \mathbf{K}_m^{-1} \mathbf{F}_d \quad (11)$$

which compared to expr. (9.3) shows a consistent reduction in amplitude.

In the *2.nd iteration* the static deflection \mathbf{x}_{st} must be corrected with the additional static deflection, all components at frequencies $\Omega, 2\Omega, 3\Omega, 4\Omega, \Omega_d, \Omega_d + 2\Omega, \Omega_d - 2\Omega$ must be corrected with additional terms, and additional terms at new frequencies such as $5\Omega, 6\Omega, \Omega_d + 4\Omega, \Omega_d - 4\Omega$, will appear. These new additional terms will show amplitudes that are still much smaller with respect to the 1.st iteration vibration components, thus allowing to neglect them unless they are in resonant conditions.

The development of the recursive iterations allows to calculate in the frequency domain all the vibration component amplitudes, with good accuracy, as will be shown in the following section where these amplitudes are compared with the ones determined in the frequency response curve function of the rotational speed, obtained from the trapezoidal rule integration scheme in the time domain, which was coupled with the Newton-Raphson iterative method for nonlinear analysis (as in [5]).

Summarizing due to the presence of the last term due to the open crack in eq. (6), additional terms will appear in the response at following frequencies:

- a) Due to the weight \mathbf{Mg} : 2Ω
- b) Due to the unbalance \mathbf{U} :

- Ω , 3Ω	1.st iteration
Ω , -3Ω , 5Ω	2.nd iteration
$\pm\Omega$, 3Ω , -5Ω , 7Ω	3.rd iteration
c) Due to the diagnostic force \mathbf{F}_d :	
$\pm(\Omega_d - 2\Omega)$, $\pm(\Omega_d + 2\Omega)$	1.st iteration
$\pm(\Omega_d - 4\Omega)$, $\pm(\Omega_d + 4\Omega)$, $\pm\Omega_d$	2.nd iteration
$\pm(\Omega_d - 6\Omega)$, $\pm(\Omega_d + 6\Omega)$, $(\Omega_d - 2\Omega)$, $(\Omega_d + 2\Omega)$	3.rd iteration

Let us focus on the equivalent forces due to the crack and to the diagnostic force, in order to evaluate the combination vibration amplitudes (disregarding once again any dynamic amplification factor).

In the 1.st iteration we have following amplitudes:

$$X(\Omega_d + 2\Omega) = X(\Omega_d - 2\Omega) = 1/2 \mathbf{K}_m^{-1} \Delta \mathbf{K}_2 \mathbf{K}_m^{-1} \mathbf{F}_d \quad (12)$$

and in the 2.nd iteration:

$$X(\Omega_d - 4\Omega) = X(\Omega_d + 4\Omega) = X(\Omega_d) = 1/4 \mathbf{K}_m^{-1} \Delta \mathbf{K}_2^* \mathbf{K}_m^{-1} \Delta \mathbf{K}_2 \mathbf{K}_m^{-1} \mathbf{F}_d \quad (13)$$

The last component in the 2.nd iteration is an additional vibration at frequency Ω_d . Therefore, the original values of $x_{1d}(\Omega_d)$ should be updated. This can be done in the iterative procedure, but it can be seen that this additional component amplitude is so small that it can easily be neglected.

Interesting to notice is that all these vibration component amplitudes due to the diagnostic force, are proportional not only to the exciting force amplitude, obviously, but also to increasing powers of the product $\mathbf{K}_m^{-1} \Delta \mathbf{K}_2$ which for small transverse cracks is of the order of 1-2 %. These combination frequency components will result extremely small, therefore it will be difficult to exploit the feature of these combination frequency vibration components, as will be shown in the following.

To demonstrate the above statements, the model of the test rig rotor of [5] will be used.

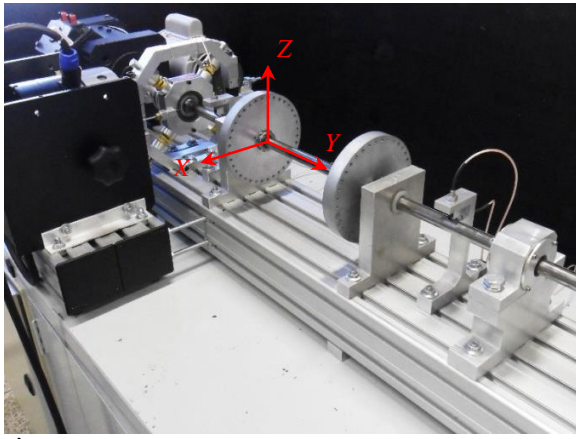
3 Rotor test rig

Figure 2a shows the rotor test rig used to represent the analyzed rotor system, and Figure 2b the finite element model of the system. The shaft has been modelled with 33 finite elements (Timoshenko's beam elements with 4 degrees of freedom per node). The rotor is composed of a flexible steel shaft (length 860 mm, diameter 17 mm) two rigid discs D_1 (node #13) and D_2 (node #23), (both with 150 mm diameter and 20 mm thickness), and two self-aligning ball bearings (B_1 and B_2 , located at nodes #4 and #31, respectively).

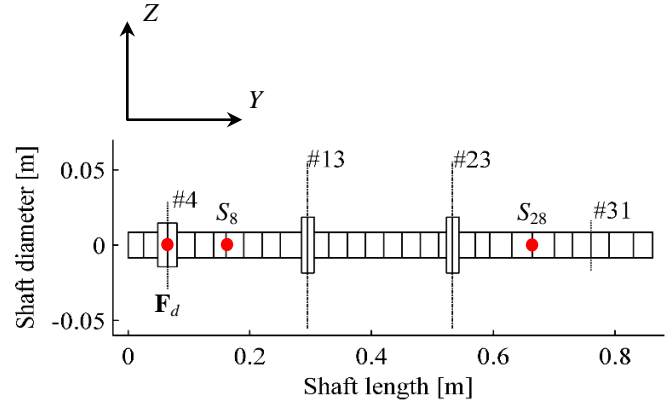
Displacement sensors are mounted at nodes #8 (S_{8X} horizontal and S_{8Z} vertical) and #28 (S_{28X} and S_{28Z}) to measure the shaft vibration. The system is driven by an electric DC motor.

The diagnostic force is applied in horizontal direction in correspondence of the bearing B_1 .

A model updating procedure was used to obtain a representative FE model, considering the rotor system without crack. A heuristic optimization technique (Differential Evolution) was used to determine the unknown parameters of the model, namely the stiffness and damping coefficients of the bearings, the proportional damping added to D (coefficients γ and β ; $D_p = \gamma \mathbf{M} + \beta \mathbf{K}$), and the angular stiffness k_{ROT} of the coupling between the electric motor and the shaft (added according the orthogonal directions X and Z of the node #1). The proposed identification process was performed 10 times, considering 100 individuals in the initial population of the optimizer. However, in this case only the regions close to the peaks associated with the natural frequencies were taken into account. Table 1 summarizes the parameter values determined at the end of the minimization process. Figure 3 presents the Campbell diagram of the rotating machine obtained considering the above updated parameters.



a)



b)

Figure 2: Rotor test rig and its FE model.

Parameters	Values	Parameters	Values	Parameters	Values
$*k_X / B_1$	8.551×10^5	$*k_X / B_2$	5.202×10^7	γ	2.730
$*k_Z / B_1$	1.198×10^6	$*k_Z / B_2$	7.023×10^8	β	4.85×10^{-6}
$**d_X / B_1$	7.452	$**d_X / B_2$	25.587	$***k_{ROT}$	770.442
$**d_Z / B_1$	33.679	$**d_Z / B_2$	91.033		

* k : stiffness [N/m] ; ** d : damping [Ns/m] ; *** k_{ROT} : stiffness [N/rad].

Table 1: Parameters of the model defined by the model updating procedure.

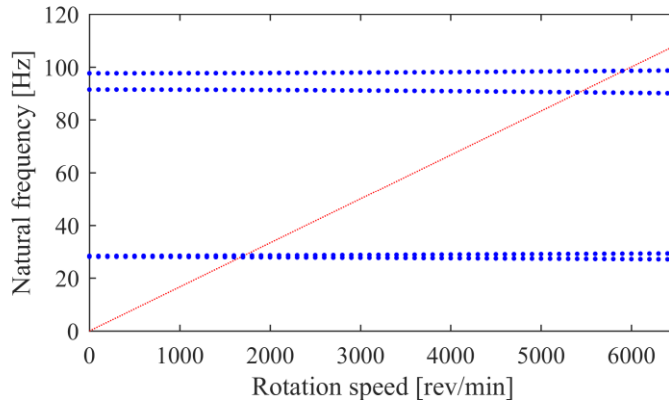


Figure 3: Campbell diagram of the test rig rotor.

From the Campbell diagram the forward whirl natural frequencies resulted to be respectively 28.5 Hz (or 1715 rpm 1.st critical speed) and 98.5 Hz (or 5910 rpm 2.nd critical speed).

It is worth mentioning that the first five natural frequencies of the cracked rotor operating at 1200 rev/min are given by (frequencies in Hz): $26.46 \leq \Omega_{1n} \leq 26.71$, $27.85 \leq \Omega_{2n} \leq 28.14$, $91.03 \leq \Omega_{3n} \leq 91.34$, $97.43 \leq \Omega_{4n} \leq 97.62$, and $123.76 \leq \Omega_{5n} \leq 123.84$. The natural frequencies are split in forward and backward whirl frequencies and the range of variation of each natural frequency is due to the different values of the cracked shaft stiffness according to the two main inertia axes of the cracked cross section, namely $(\mathbf{K}_m + \Delta\mathbf{K}_2)$ and $(\mathbf{K}_m - \Delta\mathbf{K}_2)$.

In the following we focus for simplicity on mean values of the natural frequencies: let consider the first natural frequency close to 27.0 Hz and the second close to 94.0 Hz. Resonance will occur in small frequency ranges around these values.

4 Numerical results

Figure 4 compares the vibration responses of the rotating machine (measuring plane S_{28}) determined by using the harmonic balance approach and the trapezoidal rule scheme for integration. This analysis was performed for the rotor under two different structural conditions. The first one comprises the shaft with a crack located at the element #18 with 25% depth. The second test was performed for the shaft with a crack located at the same element with 50% depth. The operational rotation speed of the rotor Ω_d was fixed at 1200 rev/min and the unbalance forces were disregarded in this case. The diagnostic force was applied along the X direction at the node #4 of the FE model, corresponding to the 1.st bearing of the shaft B_2 at a frequency $\Omega_d = 2\Omega - \Omega_n = (40 - 28.5) \text{ Hz} = 11.5 \text{ Hz}$, and amplitude of 25 N, in order to excite combination vibrations at a frequency that is close to the 1.st natural frequency). Note that the vibration responses obtained with the 2 approaches are very close, thus validating the formulation based on the harmonic balance approach. The responses determined along the plane S_8 are similar to the previous ones.

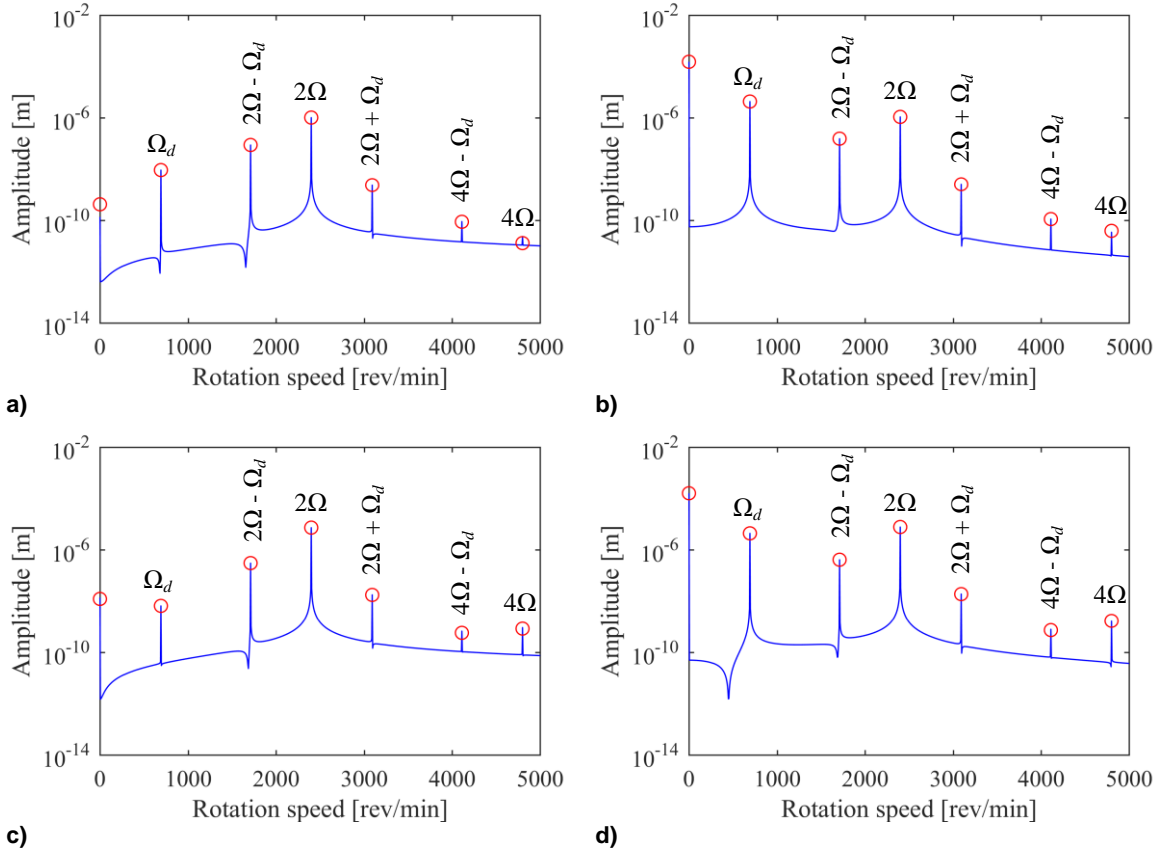


Figure 4 – Vibration responses of the cracked rotating shaft (— time integration; ○ harmonic balance):
a) 25% crack depth / S_{28X} ; b) 25% crack depth / S_{28Z} ; c) 50% crack depth / S_{28X} ; d) 50% crack depth / S_{28Z} .

Analysing the results of the rotor with the 25% crack depth following comments can be drawn: the only significant vibration amplitudes are the 2Ω components due to the crack and the weight, and the $2\Omega - \Omega_d$ component due to the crack and the diagnostic force, both roughly equal in vertical and horizontal directions, and the Ω_d component due to the diagnostic force, obviously only in horizontal direction. The $2\Omega - \Omega_d$ component is very close to the first natural frequency, therefore the amplitude is rather high, despite the fact that excitation is rather small, as shown by eq. (12). The $2\Omega + \Omega_d$ component, which has the same excitation amplitude of the $2\Omega - \Omega_d$ component is instead small because its frequency is far away from resonant frequency. All other components are at least one or two orders of magnitude smaller, as could have been forecasted from eq. (13).

Similar results have been obtained simulating the behaviour of the shaft with the 50% deep crack, with the only obvious difference that the excitation of all components related to the crack is higher.

Summarizing Fig. 5 shows that, for the considered test case, the amplitudes of the combination vibrations are too small ($< 1.0 \mu\text{m}$) to be considered as significant crack symptom, despite the fact that the highest peak at $2\Omega - \Omega_d$ is exciting the shaft first natural frequency. This might affect the applicability of the considered dynamic phenomenon in crack detection or identification techniques, as proposed by some authors. As mentioned, the problem consists in determining the amplitude and frequency of the diagnostic forces to generate measurable peaks along the vibration spectrum at the combination resonances. Since the system under consideration is linear, the vibration responses are proportional to the amplitude of the diagnostic force: doubling the diagnostic force amplitude also the combination vibrations amplitudes will be doubled, as will be shown in the following. Further the responses could be higher if we could apply the diagnostic force closer to the crack and with a frequency closer to the 1st natural frequency of the cracked shaft. Thus, higher vibrations can be excited in the middle of the shaft, where the crack is located.

Figure 5 presents the vibration responses of the rotor obtained by the sensor S_{28Z} at the combinations frequencies: $2\Omega + \Omega_d$, $2\Omega - \Omega_d$, varying Ω_d from 0 to 85 Hz in steps of 0.1 Hz. The diagnostic forces were applied always at the first bearing (B1) of the model with 25 N, 50 N, and 100 N of amplitude, separately. These tests were performed for the shaft with a crack always located at the same element, and with a depth 50% of the shaft diameter. The green line in the diagrams indicates the assumed threshold ($1.0 \mu\text{m}$) of vibration detectability in field or in laboratory.

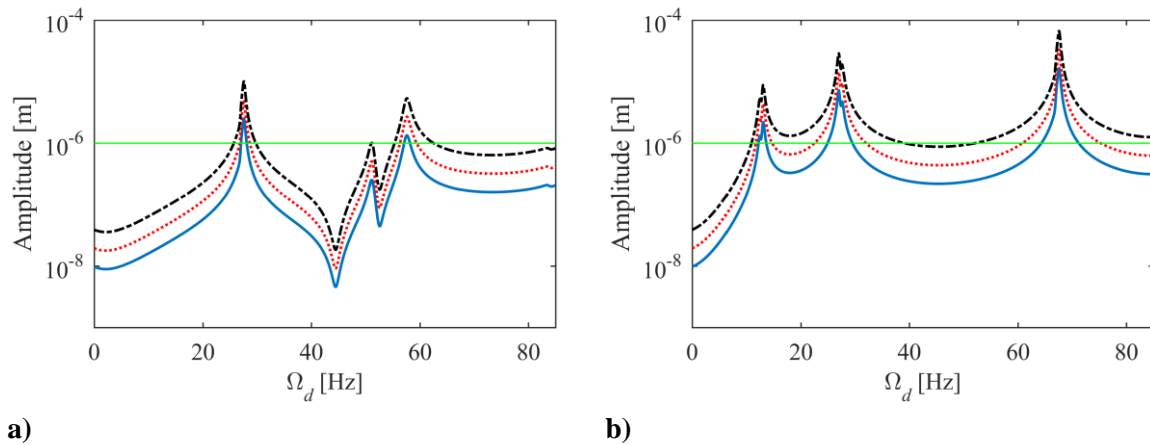


Figure 5–Different combination frequency components obtained by sensor S_{28Z} as function of Ω_d (— $F_{1d} = 25 \text{ N}$; - - - $F_{1d} = 50 \text{ N}$; - . - . $F_{1d} = 100 \text{ N}$): a) $2\Omega + \Omega_d$; b) $2\Omega - \Omega_d$

Analysing the $2\Omega + \Omega_d$ combination frequency vibrations (Fig. 5a) it results that they are excited consistently when the diagnostic force is in resonance (at 27.0 Hz) even if the combination vibrations are not in resonance, as previously announced. The second peak at 54 Hz is due to the resonant condition of the combination frequency vibration ($54 + 40 = 94$) with the second mode of vibration at 94 Hz. Linearity of the combination frequency response with the exciting diagnostic force is also confirmed.

Considering the $2\Omega - \Omega_d$ combination frequency vibrations (Fig. 5b) the diagram shows a first peak at 13.0 Hz due to the resonance of the resulting vibration ($40 - 13 = 27$), a second peak due again to the excitation in resonance (as in Fig. 5a), but with higher amplitude with respect to Fig. 5a, due to the fact that the resulting combination vibration is at frequency 13 Hz, below the resonance, whilst in Fig. 5a the resulting frequency was at 67 Hz, above the resonance. Finally a 3.rd peak arises at 67 Hz due to another resonant condition with the 1.st natural frequency ($67 - 40 = 27$). Other combination frequency vibrations are too small to be considered as significant symptoms of the presence of the crack.

Interesting is also to analyse the trend of the phase with respect to the exciting diagnostic force of the combination vibrations as function of the diagnostic excitation frequency.

Figure 6 presents the phase angle of the rotor vibration responses obtained by the sensor S_{28Z} at the combination frequencies $2\Omega + \Omega_d$ and $2\Omega - \Omega_d$, varying Ω_d from 0 to 85 Hz in steps of 0.1 Hz. In this case, the diagnostic force was applied as previously in horizontal direction with an amplitude of 100 N. The rotor operational speed Ω_d was as previously fixed to 1200 rev/min. These phase diagrams were determined for the shaft with a crack located at the element #10 with 25% depth, as well as for the case with a crack located at the element #10 with 50% depth, and finally for a crack located at the element #18 with 50% depth.

In Fig. 6a phase variations from 0° to -180° can be noticed in correspondence of the two peaks shown in Fig. 5a, as could be expected when passing resonant conditions. In Fig 6b instead the phase variations go in opposite way (from 0° to $+180^\circ$) when crossing resonances: this must be due to the sign of the diagnostic frequency in the combination frequency. Significant changes in the phase behavior arise only due to changes in crack position along the shaft and do not appear when changing the depth of the crack only.

These phase trends as function of the exciting frequency could also help in detecting cracks in rotating machinery to which external diagnostic forces are applied.

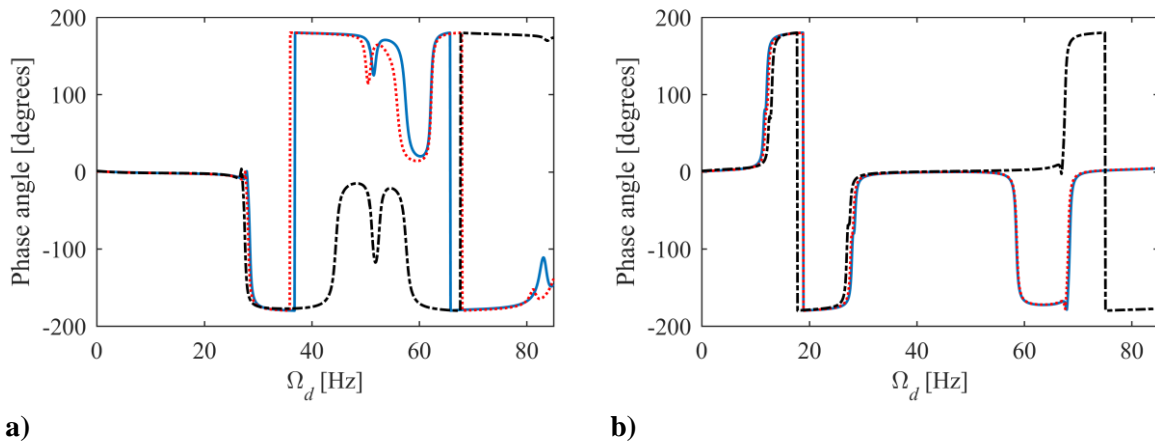


Figure 6 – Phase angles of combination vibrations obtained by the sensor S_{28Z} as function of Ω_d
 (— element #10 with 25% depth; - - - element #10 with 50% depth; - . - . element #18 with 50% depth)
 a) $2\Omega + \Omega_d$; b) $2\Omega - \Omega_d$.

5. Conclusions

A possible technique for detecting cracks in rotating machinery consists in applying additional external forces at frequencies, different from rotational speed, in order to generate so called combination frequency vibrations, that appear only in presence of transverse cracks. In order to generate vibrations that can emerge from noise, the combination frequency vibrations should be in resonance with some natural frequency of the shaft. This can be obtained with a suitable frequency of the exciting force. In order to analyse the conditions for exciting combination frequency vibrations with sufficient amplitude an original approach based on the harmonic balance method in the frequency domain is proposed in this paper. The approach is validated by comparing the obtained spectral amplitudes with the rotational frequency response curve obtained by time integration of the original non-linear equation of motion. Through the development of the harmonic balance approach simple expressions for the combination frequency vibration amplitudes are derived that allow to analyse the mechanism of combination frequency vibration generation. The development of the different combination frequency components allows in general to neglect and skip all components except the first components that only have sufficient amplitudes to be recognized and used for crack detection. The numerical simulation of a test rig model cracked rotor confirms the forecasted situation. The harmonic balance approach allows further to evaluate for each combination frequency component the amplitude as function of the excitation frequency. Thus, the applicability of the combination frequency excitation for crack detection in rotating machinery has been analysed.

Acknowledgments

The authors are thankful to the financial support provided to the present research effort, by CNPq (574001/2008-5) and FAPEMIG (TEC-APQ-3076-09 / TEC-APQ-02284-15), through the INCT-EIE.

References

- [1] Bachschmid, N., Pennacchi, P., and Tanzi, E., *Cracked Rotors: A Survey on Static and Dynamic Behaviour Including Modelling and Diagnosis*, 2010, Springer-Verlag, Berlin, Germany.
- [2] Bently, D.E. and Hatch, C.T., *Fundamentals of Rotating Machinery Diagnostics*, Bently Pressurized Bearing Company, 2002, Minden, NV, USA.
- [3] Mani, G., Quinn, D.D., and Kasarda, M., *Active Health Monitoring in a Rotating Cracked Shaft using Active Magnetic Bearings as Force Actuators*, Journal of Sound and Vibration, 2006, Vol. 294, No. 1, pp. 454-465.
- [4] Ishida, Y. and Inoue, T., *Detection of a Rotor Crack Using a Harmonic Excitation and Nonlinear Vibration Analysis*, Journal of Vibration and Acoustics, 2006, Vol. 128, No. 1, pp. 741-749.
- [5] Cavalini Jr, A.A., Sanches, L., Bachschmid, N., and Steffen Jr, V., *Crack Identification for Rotating Machines Based on a Nonlinear Approach*, Mechanical Systems and Signal Processing, 2016, Vol. 1, No. 1, pp. 1-14.
- [6] Mayes, I.W. and Davies, W.G.R., *Analysis of the Response of a Multi-Rotor-Bearing System Containing a Transverse Crack in a Rotor*, Journal of Vibration, Acoustics, Stress and Reliability in Design, 1984, Vol. 106, No. 1, 0 pp. 139-145.
- [7] Cavalini Jr, A. A., Lara-Molina, F.A., Sales, T.P., Koroishi, E.H., and Steffen Jr, V., *Uncertainty Analysis of a Flexible Rotor Supported by Fluid Film Bearings*, Latin American Journal of Solids and Structures, 2015, Vol. 12, No. 8, pp. 1487-1504.